

A Spectro- and Conductometric Study of the Reaction of Imidazoline-2-selone Derivatives with Bromine – Crystal Structure of 1,2-Bis(3-methyl-4-imidazolin-2-ylum dibromoselenanide)ethane

Francesco Bigoli^a, Paola Deplano^b, Francesco A. Devillanova^b, Vito Lippolis^{*b}, Maria Laura Mercuri^{*b}, Maria Angela Pellinghelli^a and Emanuele F. Trogu^b

Dipartimento di Chimica Generale ed Inorganica, Chimica Analitica, Chimica Fisica, Università degli Studi di Parma^a, Viale delle Scienze 78, I-43100 Parma, Italy

Dipartimento di Chimica e Tecnologie Inorganiche e Metallorganiche, Università degli Studi di Cagliari^b, Via Ospedale 72, I-09124 Cagliari, Italy
E-mail: mercuri@vaxca1.unica.it, lippolis@vaxca1.unica.it

Received June 23, 1997

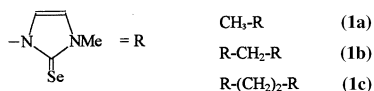
Keywords: Bromine / Imidazoline-2-selone / Hypervalent Se compounds / Dications

The oxidative addition of Br₂ to the imidazoline-2-selone derivatives **1a–c** has been studied by spectrophotometric and conductometric techniques. The experimental results clearly indicate that this reaction involves the dications **2a–c**, containing an Se–Se bond, as intermediates in the formation of

the hypervalent 10-Se-3 selenium compounds **3a–c** containing the Br–Se–Br group. The crystal structure of 1,2-bis(3-methyl-4-imidazolin-2-ylum dibromoselenanide)ethane (**3c**), a new stable hypervalent 10-Se-3 compound, is also reported.

Introduction

In recent years, a great deal of synthetic and structural characterization work has been carried out on the products of the reactions of the donors **1a–c**, containing the imidazoline-2-selone ring, with acceptors such as diiodine,^[1] interhalogens (IBr and ICl)^[2] and unsaturated polynitriles (TCNQ).^[3]



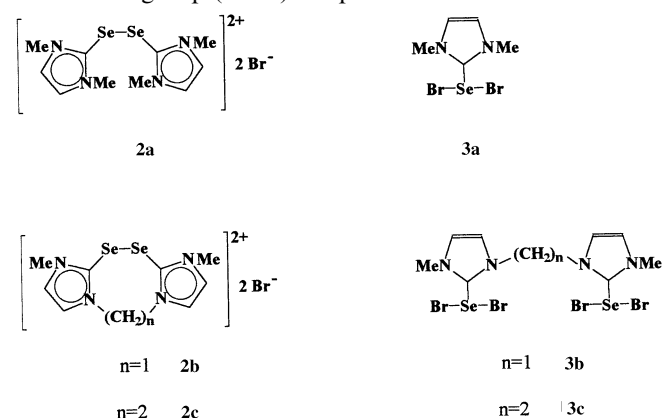
A variety of products has been obtained including neutral adducts, dications containing the Se–Se bridge, and hypervalent 10-Se-3^[4] compounds containing the I–Se–I group.

While addition of I₂ to **1a** and **1c** quantitatively produces the I–Se–I insertion derivatives, the corresponding reaction of Br₂ with **1a** has recently been reported^[5] to give the analogous Br–Se–Br insertion derivative **3a** with a 1:1 **1a**/Br₂ molar ratio and an ionic compound with a 1:0.5 **1a**/Br₂ molar ratio. This latter has been hypothesized to be 2,2'-diselenobis(1,3-dimethyl-4-imidazolinium) dibromide (**2a**) on the basis of previous studies carried out by Arduengo and Burgess^[6] on the oxidative addition complexes of the sulfur analogue of **1a** with Br₂. However, we have previously obtained **2a** by reacting **1a** with IBr in a 1:1 molar ratio and have reported its structural characterization.^[2] In order to ascertain whether **1b** and **1c** show the same behavior as **1a** in the reaction with bromine, and whether dications containing the Se–Se bridge are intermediates in the formation of the hypervalent compounds, a spectro-

photometric and a conductometric study of this reaction has been undertaken. The X-ray crystal structure of 1,2-bis(3-methyl-4-imidazolin-2-ylum dibromoselenanide)ethane (**3c**) is also reported.

Results and Discussion

Upon reaction of **1a–c** with 0.5 equiv. of molecular bromine in CH₃CN, ionic compounds consisting of dications containing the Se–Se bridge and Br[–] counterions (**2a–c**) are obtained. When 1 equiv. of Br₂ per selenium atom is used, hypervalent selenium compounds featuring the Br–Se–Br group (**3a–c**) are produced.



As mentioned above, we have previously obtained compound **2a** by the reaction of **1a** with IBr and have reported its X-ray structural characterization.^[2] The crystal structure of **3a** was recently determined by Williams et al.^[5] while this study was being carried out. The reported data are consistent with the crystal data of the sample isolated by us.

Single crystals suitable for X-ray studies have also been obtained for **3c**. The crystallographic data are given in Table 1, the geometrical parameters are listed in Table 2. The structural data of **3c** are in good agreement with those of the corresponding iodo derivative.^{[1][7][8]} In fact, the molecule (Figure 1) shows a pseudo two-fold axis and a *gauche* conformation [N(11)–C(41)–C(42)–N(12) 59(1)°]; the Br–Se–Br fragments are asymmetric [Se(11)–Br(11) 2.662(2), Se(11)–Br(21) 2.521(2), Se(12)–Br(12) 2.650(3), Se(12)–Br(22) 2.531(4) Å], essentially linear [Br(11)–Se(11)–Br(21) 175.7(1)°, Br(12)–Se(12)–Br(22) 172.1(1)°], and roughly perpendicular to the corresponding imidazoline ring [the values of the Br–Se–C–N torsion angles are in the –101(1) to 78(1)° range]. The dihedral angle between the two imidazoline rings is 46.6(5)°. The Se atoms show a roughly square-planar coordination due to the very appreciable interactions Se(11)⋯Br(21) (*x*, –*y*, *z* – 1/2) 3.344(3) Å and Se(12)⋯Br(22) (*x*, –*y*, 1/2 + *z*) 3.754(3) Å. These interactions are responsible for the formation of chains in the directions of *c* through the axial glide plane. The chains are held together by weak interactions of the type Br⋯C and C⋯C (Figure 2). The structure shows considerable similarities with those of **2a**^[5] and SeBr₂tmtu^[9].

Figure 1. ORTEP view of **3c**; thermal ellipsoids are drawn at a 30% probability level

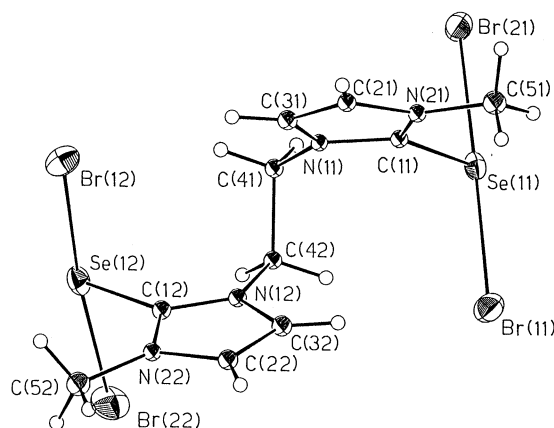


Figure 2. Projection of the structure of **3c** along [001]

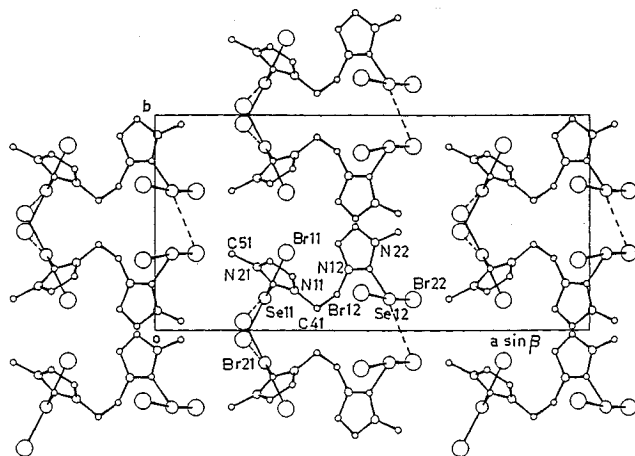


Table 1. Crystallographic data of **3c**: C₁₀H₁₄Br₄N₄Se₂

formula	C ₁₀ H ₁₄ Br ₄ N ₄ Se ₂
molecular mass [g/mol]	667.78
crystal system	monoclinic
space group	<i>Cc</i>
<i>a</i> [Å]	21.399(5)
<i>b</i> [Å]	10.619(6)
<i>c</i> [Å]	8.090(7)
β [°]	90.72(2)
<i>U</i> [Å ³]	1838(2)
<i>Z</i>	4
<i>d_c</i> [g cm ^{–3}]	2.413
diffractometer	Philips PW 1100
radiation	graphite-monochromated
wavelength	Mo- <i>K_α</i> (λ = 0.71073 Å)
<i>F</i> (000)	1240
<i>T</i> [K]	295
crystal size [mm]	0.11 × 0.56 × 0.62
μ [cm ^{–1}]	127.13
scan mode	θ–2θ
scan speed [° min ^{–1}]	3–9.6
scan width [°]	1.20 + 0.345 tan θ
θ range for intensity collection [°]	3–30
data collected	± <i>h</i> , <i>k</i> , <i>l</i>
no. of measured reflections	2844
no. of reflections with <i>I</i> ≥ 2σ(<i>I</i>)	2090
no. of refined parameters	180
min./max. height in final Δρ map [e Å ^{–3}]	–0.51/1.70
<i>R</i> = Σ (Δ <i>F</i>) /Σ <i>F_o</i>	0.0549
<i>wR</i> = [Σ <i>w</i> (Δ <i>F</i>) ² /Σ <i>wF_o</i> ²] ^{1/2}	0.0692
<i>k</i> , <i>g</i> (<i>w</i> = <i>k</i> /[σ ² (<i>F_o</i>) + <i>gF_o</i> ²])	1.5042, 0.001495

Table 2. Bond lengths [Å] and angles [°], with e.s.d.'s in parentheses, of **3c**: C₁₀H₁₄Br₄N₄Se₂

bond lengths [Å]			
Se(11)–Br(11)	2.662(2)	N(21)–C(51)	1.45(2)
Se(11)–Br(21)	2.521(2)	N(12)–C(12)	1.30(2)
Se(11)–C(11)	1.95(1)	N(12)–C(32)	1.39(2)
Se(12)–Br(12)	2.650(3)	N(12)–C(42)	1.47(2)
Se(12)–Br(22)	2.531(4)	N(22)–C(12)	1.39(2)
Se(12)–C(12)	1.88(1)	N(22)–C(22)	1.40(2)
N(11)–C(11)	1.37(2)	N(22)–C(52)	1.45(2)
N(11)–C(31)	1.37(2)	C(21)–C(31)	1.34(2)
N(11)–C(41)	1.43(2)	C(41)–C(42)	1.56(2)
N(21)–C(11)	1.35(2)	C(22)–C(32)	1.34(2)
N(21)–C(21)	1.39(2)		
bond angles [°]			
Br(21)–Se(11)–C(11)	88.2(4)	C(22)–N(22)–C(52)	127.8(12)
Br(11)–Se(11)–C(11)	88.1(4)	C(12)–N(22)–C(52)	127.0(12)
Br(11)–Se(11)–Br(21)	175.7(1)	C(12)–N(22)–C(22)	105.1(10)
Br(22)–Se(12)–C(12)	88.8(4)	N(11)–C(11)–N(21)	107.2(11)
Br(12)–Se(12)–C(12)	83.3(4)	Se(11)–C(11)–N(21)	126.0(9)
Br(12)–Se(12)–Br(22)	172.1(1)	Se(11)–C(11)–N(11)	126.8(9)
C(31)–N(11)–C(41)	125.1(11)	N(21)–C(21)–C(31)	107.4(12)
C(11)–N(11)–C(41)	126.4(11)	N(11)–C(31)–C(21)	108.4(12)
C(11)–N(11)–C(31)	108.5(10)	N(11)–C(41)–C(42)	111.9(10)
C(21)–N(21)–C(51)	125.7(12)	N(12)–C(12)–N(22)	108.7(11)
C(11)–N(21)–C(51)	125.8(12)	Se(12)–C(12)–N(22)	124.5(8)
C(11)–N(21)–C(21)	108.4(10)	Se(12)–C(12)–N(12)	126.7(11)
C(32)–N(12)–C(42)	124.6(11)	N(22)–C(22)–C(32)	109.8(13)
C(12)–N(12)–C(42)	124.8(11)	N(12)–C(32)–C(22)	105.6(11)
C(12)–N(12)–C(32)	110.6(11)	N(12)–C(42)–C(41)	111.5(10)

In the low-frequency region, the FT-Raman spectra of **3a–c** each show two strong peaks at 187 ± 6 and 152 ± 6 cm^{–1}, attributable to ν_{as} and ν_s of the Br–Se–Br three-body system, respectively.^{[5][9][10]} Similarities are also ob-

served in the FT-Raman spectra of **2a** and **2c**; thus, the peaks at 248 and 189 cm^{-1} for **2c** must be in part associated with the $\nu(\text{Se}-\text{Se})$ vibration, in accordance with the findings for **2a** and other dications.^[2] The FT-Raman spectrum of **2b** is more complicated and, in addition to the peaks at 250 and 187 cm^{-1} (the intensities of which are reversed compared to those found for **2a** and **2c**), shows one strong peak at 176 cm^{-1} . This spectrum could be explained by hypothesizing that in **2b** some dication units interact strongly with Br^- ions forming an $\text{Se}-\text{Se}-\text{Br}$ three-body system, which could be vibrationally described as a Br_3^- unit. In fact, for an only slightly asymmetric Br_3^- anion, the symmetric stretching vibration ν_1 is found near 160 cm^{-1} and the antisymmetric ν_3 near 190 cm^{-1} .^{[10][11]} From this, it follows that the peak at 176 cm^{-1} could be assigned to the ν_1 mode of the $\text{Se}-\text{Se}-\text{Br}$ group, while the increased intensity of the peak at 187 cm^{-1} is most likely attributable to the contribution from the ν_3 antisymmetric vibration of the $\text{Se}-\text{Se}-\text{Br}$ group.

In order to ascertain whether the aforementioned dications are intermediates in the formation of the hypervalent selenium compounds, we have investigated the oxidative addition of Br_2 in CH_3CN solution by UV/visible spectroscopy and conductometric measurements.

The addition of increasing amounts of Br_2 to CH_3CN solutions of **1a**, **1b** or **1c** produces a drastic change in the electronic spectra of the free ligands; the main features are similar in the three cases and, as shown in Figure 3a for **1c**, two well-defined isosbestic points are observed at 291 and 301 nm indicating an initial conversion of the free ligand into a new species up to a 1:1 **1c**/ Br_2 molar ratio and subsequent transformation of this species once its formation is completed. A spectrum identical to that recorded for the 1:1 **1c**/ Br_2 solution is obtained from a CH_3CN solution of **2c**; thus, the formation of the dication is unequivocally proven when working at this molar ratio. The dication undergoes a further transformation upon increasing the amount of bromine to a 1:2 **1c**/ Br_2 molar ratio, leading to **3c** as shown by the UV/Visible spectrum of **3c** compared with that recorded on the 1:2 **1c**/ Br_2 solution. The spectral features of **3a-c** are very similar to those of a tribromide due to the great similarity of the chromophores $\text{Br}-\text{Se}-\text{Br}$ and $[\text{Br}-\text{Br}-\text{Br}]^-$.^[12] In Figure 3b, a plot of the absorbance at 260 nm versus the **1c**/ Br_2 molar ratio is depicted; it shows that the formation of **2c** and subsequently of **3c** is quantitative. A similar plot is observed for **1b**, whereas for **1a** less evident equivalence points at the 1:0.5 and 1:1 **1a**/ Br_2 ratios might suggest that the formation of the dication and of the hypervalent compound are equilibrium reactions. In order to further support the hypothesis that dications **2a-c** are intermediates in the formation of the hypervalent compounds **3a-c**, another experiment was carried out in which increasing amounts of Br_2 were added to CH_3CN solutions of **2a-c**; the resulting UV/visible spectra indeed showed that the hypervalent compounds were formed.

The oxidative addition of bromine to **1a-c** has also been investigated by conductometric measurements. The conduc-

tivities of CH_3CN solutions of the free ligands were monitored during stepwise Br_2 addition. Figure 4 shows plots of the molar conductivities versus the Br_2/L molar ratios; formation of an ionic species is clearly evident from the increase in the conductivity values up to a 1:1 Br_2/L (1:0.5 for **1a**) molar ratio. This species disappears upon the addition of further Br_2 and conductivity reaches a minimum value at a 2:1 Br_2/L (1:1 for **1a**) molar ratio. The UV/visible spectra of the solutions at the 1:1 and 2:1 Br_2/L (**L** = **1b**, **1c**) molar ratios, respectively, showed the corresponding dications and hypervalent compounds to be the only species present. The conductometric titration of **1a**, on the other hand, indicates an equilibrium reaction between the three species **1a**, **2a** and **3a**, in line with the spectrophotometric evidence.

Figure 3. 3a: UV/Vis spectra at 293 K in a 0.1-cm silica cell of CH_3CN solutions containing fixed amounts of **1c** ($[\text{1c}] = 2.5 \times 10^{-4} \text{ mol l}^{-1}$) and variable Br_2 concentrations in the ratios: (a) 1:0; (b) 1:0.2; (c) 1:0.4; (d) 1:0.6; (e) 1:0.8; (f) 1:1; (g) 1:1.2; (h) 1:1.4; (i) 1:1.6; (l) 1:2. — 3b: Plot of the absorbances of the same CH_3CN solutions of **1c** and Br_2 as in (3a) versus $[\text{1c}]/[\text{Br}_2]$ molar ratios at $\lambda = 260 \text{ nm}$. The increase in absorbance over the 1:2 **1c**/ Br_2 molar ratio could be attributed to the presence of Br_3^- in the Br_2 solution used for the titration. In fact, in Br_2 solutions with concentrations ranging from 1×10^{-3} to $2.5 \times 10^{-3} \text{ mol l}^{-1}$, about 1–2% of Br_3^- is observed

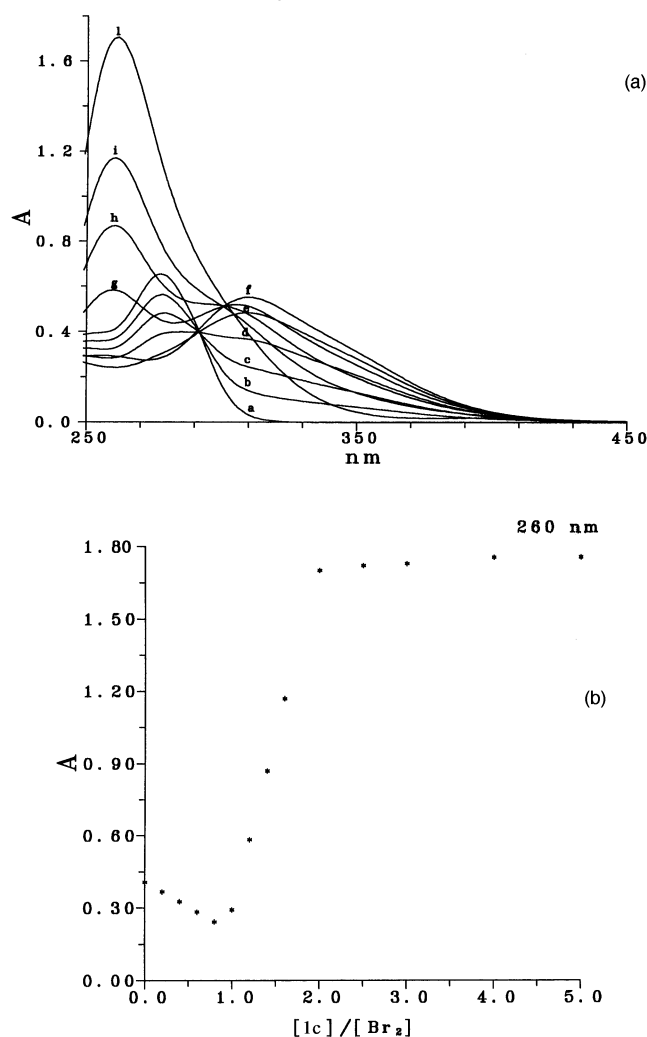
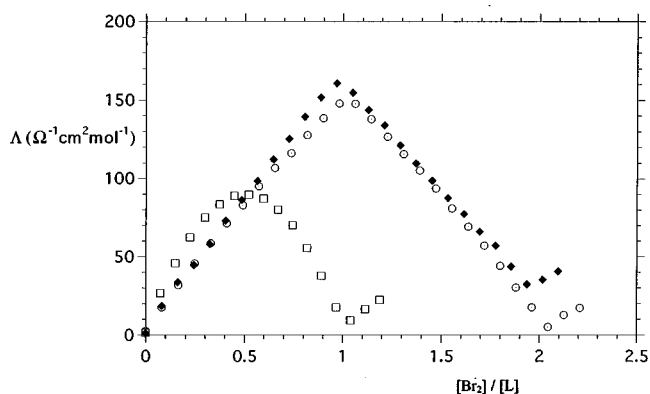


Figure 4. Plots of the molar conductivities recorded during the titrations of **1a–c** {[**1a**] = 2.16×10^{-3} mol l⁻¹ (□); [**1b**] = 1.06×10^{-3} mol l⁻¹ (○); [**1c**] = 1.99×10^{-4} mol l⁻¹ (◆)} with Br₂ ([Br₂] = 9.61×10^{-3} ; 1.04×10^{-2} ; 1.93×10^{-3} mol l⁻¹ for **1a–c**, respectively) versus the [Br₂]/[L] molar ratios



The observed reactions of **1a–c** with Br₂ are in good agreement with their electrochemical behavior. To confirm the tendency of the three ligands to undergo oxidation we also carried out an electrochemical study in CH₂Cl₂ solution (**2a–c** and **3a–c** are also obtained using CH₂Cl₂ as the solvent instead of CH₃CN; the electrochemical measurements were performed in CH₂Cl₂ for solubility reasons). In fact, cyclic voltammograms scanned in the anodic direction and reversed at +1.0 and -0.2 V to the starting potential (0.0 V), show two irreversible oxidations and one irreversible reduction for **1a** and **1c**, while only one broad oxidation peak and one reduction peak are observed for **1b** (see Table 3). When the scans are performed in the cathodic direction, the reduction peak does not appear for all ligands. This peak could therefore be attributed to the reduction of the oxidation products. The two oxidation peaks may be related to a two-step process involving the initial oxidation of one Se atom, which then interacts with either the unoxidized Se atom of the same molecule in the case of **1b** and **1c**, or with the Se atom of a different molecule in the case of **1a**. Subsequently, according to a simplified molecular orbital description for the Se–Se bond formation, this intermediate has one electron in the antibonding molecular orbital, which is removed in the second oxidation step to give the Se–Se dication.

Table 3. Anodic peak (*Epa*) and cathodic peak potentials (*Epc*) determined by cyclic voltammetry in CH₂Cl₂ for **1a–c** (1×10^{-3} mol l⁻¹). Pt electrode vs. SCE (saturated calomel electrode) in the presence of Bu₄NBF₄ (1×10^{-1} mol l⁻¹). Scan rate: 100 mV s⁻¹

L	<i>Epa</i> ₁ (V)	<i>Epa</i> ₂ (V)	<i>Epc</i> (V) ^[a]
1a	+0.57	+0.75	+0.08
1b	+0.60	+0.73	+0.24
1c	+0.50	+0.66	+0.04

^[a] These peaks do not appear when scanning is started in the cathodic direction.

Conclusions

In this paper, we have reported the structure of the hypervalent Se compound obtained by oxidative addition of Br₂ to **1c** (**3c**). Hypervalent 10-Se-3 compounds of this type are quite uncommon, **3a**,^[5] 1,3-diisopropyl-4,5-dimethyl-4-imidazolin-2-ylum diiodoselenanide^[7] and the diiodoselenanides obtained from **1a** and **1c**^[1] being the only such compounds structurally characterized to date. We have also demonstrated that the reactions of **1a–c** with bromine leading to the hypervalent compounds are two-step oxidation processes involving as intermediates the dications (**2a–c**), which contain Se–Se bridges. It is relevant that such dications are not formed in the reaction of **1a–c** with diiodine,^[1] neither in solution nor in the solid state, whatever the molar ratio of reactants used. Only in the case of the reaction of diiodine with the saturated analogue of **1a**, i.e. *N,N'*-dimethylimidazolidine-2-selone, was formation of the corresponding dication observed; the solid product was found to be a mixed-valence compound containing equimolecular amounts of the CT complex and the dication having two triiodides as counterions.^[13] Finally, while **1a–c** show the same behavior in the reaction with bromine, the reaction with diiodine is more selective since different products are obtained from these rather similar donors.

The Ministero della Università e Ricerca Scientifica e Tecnologica of Italy (MURST 40%, Reattività e Catalisi) is acknowledged for support in this research.

Experimental Section

Materials: Reagents and solvents of reagent grade purity were used as received from Aldrich. The compounds **1a–c** were prepared as described previously.^[1]

Compounds 2a–c and 3a–c: The compounds **3a–c** were prepared by leaving to stand CH₃CN solutions of the ligands and Br₂ in a 1:1 (for **1a**) or 1:2 (for **1b** and **1c**) molar ratio at room temperature. After several days, well-shaped yellow-orange crystals of **3c** suitable for X-ray diffraction studies and yellow-orange crystals of **3a** and **3b** were obtained. Yields of each compound were typically 70%. The compounds **2a–c**, obtained as yellow microcrystals, were prepared analogously using a 1:0.5 (for **1a**, yields 88%) or 1:1 (for **1b** and **1c**, yields 90%) molar ratio. Elemental analysis data and FT-Raman spectra for **2a** and **3a** have been reported previously.^[2]

2a: Electronic spectrum (250–550 nm): λ_{max} (ε) = 275 (22280), 312 nm (20480 l mol⁻¹ cm⁻¹).

2b: C₉H₁₂N₄Br₂Se₂: calcd. C 21.88, H 2.45, N 11.34; found C 22.09, H 2.52, N 11.39. – Raman (500–50 cm⁻¹): ν̃ = 290 (2.0), 250 (5.2), 218 (1.9), 187 (7.6), 176 (10), 135 (3.0), 128 (5.0), 92 (3.4), 74 (3.4). – Electronic spectrum (250–550 nm): λ_{max} (ε) = 292 nm (28200 l mol⁻¹ cm⁻¹).

2c: C₁₀H₁₄Br₂N₄Se₂ × 0.5 CH₃CN: calcd. C 25.00, H 2.96, N 11.93; found C 25.19, H 3.15, N 12.06. – Raman (500–50 cm⁻¹): ν̃ = 282 (1.0), 248 (10.0), 189 (1.3), 87 (1.1). – Electronic spectrum (250–550 nm): λ_{max} (ε) = 310 nm (19900 l mol⁻¹ cm⁻¹).

3a: Electronic spectrum (250–550 nm): λ_{max} (ε) = 260 nm (32600 l mol⁻¹ cm⁻¹).

3b: C₉H₁₂Br₂N₄Se₂: calcd. C 16.54, H 1.85, N 8.57; found C 16.77, H 1.90, N 8.64. – Raman (500–50 cm⁻¹): ν̃ = 193 (10.0),

153 (7.5), 137 (3.0), 107 (2.8), 85 (2.7). – Electronic spectrum (250–550 nm): λ_{max} (ϵ) = 262 nm (58000 l mol⁻¹ cm⁻¹).

3c: C₁₀H₁₄Br₄N₄Se₂: C 17.99, H 2.11, N 8.39; found C 18.11, H 2.17, N 9.26. – Raman (500–50 cm⁻¹): $\tilde{\nu}$ = 184 (10.0), 146 (9.4), 64 (2.5). – Electronic spectrum (250–550 nm): λ_{max} (ϵ) = 260 nm (56400 l mol⁻¹ cm⁻¹).

X-ray Data Collection and Structure Refinement: Crystallographic data are given in Table 1. The diffraction measurements were made on a Philips PW 1100 diffractometer with graphite-monochromated Mo-K α radiation (see Table 1); the data were collected using the θ – 2θ scan technique. During the data reduction, intensities were corrected for Lorentz and polarization effects. A correction for absorption was applied: maximum and minimum values for the transmission factors were 1.000 and 0.514.^{[14][15]} Solution by direct methods (SHELX-86),^[16] full-matrix least-squares refinement, and anisotropic thermal parameters for all non-hydrogen atoms were used. The H-atoms were introduced in calculated positions and refined “riding” on the corresponding atoms with unique isotropic thermal parameters [$U = 0.0725(166)$ Å²]. The weighting scheme $w = k/[\sigma^2(F_o) + gF_o^2]$ was applied, with $k = 1.5042$ and $g = 0.001495$. Scattering factors were taken from ref.^[17]. The final difference density map showed a minimum peak of -1.40 Å⁻³ and a maximum peak of 1.29 Å⁻³. Structure refinement and final geometric calculations were carried out with the SHELX-76^[18] and PARST^[19] programs. The drawing was produced using ORTEP^[20] and PLUTO.^[21]

Spectroscopic Measurements. – **FT-Raman Spectra:** FT-Raman spectra (resolution ± 4 cm⁻¹) were recorded on a Bruker RFS100 FTR spectrometer fitted with an indium-gallium arsenide detector (room temp.) and operating with an excitation frequency of 1064 nm (Nd:YAG laser). The power level of the laser source was tuned between 20–40 mW. The solid samples, in the form of powders or crystals, were packed into suitable cells and then fitted into the compartment designed for use with a 180° scattering geometry. No sample decomposition was detected during the experiments. The values given in parentheses represent the intensities of the peaks relative to the strongest, which is given a value of 10.

UV/Visible Measurements: Electronic spectra were recorded of solutions in CH₃CN (freshly distilled from CaH₂) using a Cary 5 spectrophotometer equipped with a temperature probe accessory connected to a thermostatted multi-cell block. The CH₃CN solutions of Br₂ were standardized with a standard aqueous Na₂S₂O₃ solution (0.1000 mol l⁻¹) according to traditional methods.

1a: A set of 11 solutions containing a fixed concentration of the ligand (2.50×10^{-4} mol l⁻¹) and variable Br₂ concentrations ranging from 2.50×10^{-5} to 5.00×10^{-4} mol l⁻¹ (in the ratios [1a]:[Br₂] = 1:0; 1:0.1; 1:0.2; 1:0.3; 1:0.4; 1:0.5; 1:0.6; 1:0.8; 1:1; 1:1.5; 1:2), was prepared. Spectra were recorded at $T = 20^\circ\text{C}$, in the 250–550 nm range, using 0.1-cm path length silica cells.

1b: A set of 15 solutions containing a fixed concentration of the ligand (2.50×10^{-4} mol l⁻¹) and variable Br₂ concentrations ranging from 5×10^{-5} to 1.25×10^{-3} mol l⁻¹ (in the ratios [1b]:[Br₂] = 1:0; 1:0.2; 1:0.4; 1:0.6; 1:0.8; 1:1; 1:1.2; 1:1.4; 1:1.6; 1:2; 1:2.4; 1:2.6; 1:3; 1:4; 1:5) was prepared. Spectra were recorded at $T = 20^\circ\text{C}$ in the 250–550 nm range using 1-cm path length silica cells.

1c: A set of 14 solutions containing a fixed concentration of the ligand (2.50×10^{-4} mol l⁻¹) and variable Br₂ concentrations ranging from 5.00×10^{-5} to 1.25×10^{-3} mol l⁻¹ (in the ratios [1c]:[Br₂] = 1:0; 1:0.2; 1:0.4; 1:0.6; 1:0.8; 1:1; 1:1.2; 1:1.4; 1:1.6; 1:2;

1:2.5; 1:3; 1:4; 1:5), was prepared. Spectra were recorded at $T = 20^\circ\text{C}$, in the 250–550 nm range, using 1-cm path length silica cells.

Conductometric Titrations: Conductometric titrations were carried out at $T = 25^\circ\text{C}$ in a standard thermostatted cell using solutions in CH₃CN (freshly distilled from CaH₂), with a Model 120 microprocessor conductivity meter “Analytical Control”. The k cell (1.23 cm⁻¹) was determined by measuring the conductivity of three solutions of kiln-dried (12 h) KCl (0.1, 0.01 and 0.001 mol l⁻¹, respectively) in doubly-distilled deionized water at $T = 25^\circ\text{C}$. The conductivity values were corrected for the dilution error using the multiplicative factor $f = (V + V_o)/V_o$, where V_o is the starting volume (30 ml) of the **1a**, **1b** and **1c** solutions and V is the volume of the added Br₂ solution. Conductivity was recorded 5 minutes after each Br₂ addition in order to let the temperature equilibrate to 25°C.

Electrochemistry: Cyclic voltammetry experiments were performed using a conventional three-electrode cell, consisting of a Pt counter electrode and a Pt micro-working electrode vs. SCE (saturated calomel electrode). The experiments were performed at room temperature in anhydrous CH₂Cl₂. The solution was 1×10^{-3} mol l⁻¹ in **L** (**1a**, **1b**, **1c**) with Bu₄NBF₄ (1×10^{-1} mol l⁻¹) as the supporting electrolyte. A stream of argon was passed through the solution prior to the scan. Data were recorded on a computer-controlled EG&G (Princeton Applied Research) potentiostat-galvanostat model 273 EG&G, using Model 270 electrochemical analysis software. The scan rate was 100 mV s⁻¹.

- [1] F. Bigoli, P. Deplano, F. A. Devillanova, V. Lippolis, M. L. Mercuri, M. A. Pellinghelli, E. F. Trogu, *Gazz. Chim. Ital.* **1994**, *124*, 445–454.
- [2] F. Bigoli, F. Demartin, P. Deplano, F. A. Devillanova, F. Isaia, V. Lippolis, M. L. Mercuri, M. A. Pellinghelli, E. F. Trogu, *Inorg. Chem.* **1996**, *35*, 3194–3201.
- [3] F. Bigoli, P. Deplano, F. A. Devillanova, A. Girlando, V. Lippolis, M. L. Mercuri, M. A. Pellinghelli, E. F. Trogu, *Inorg. Chem.* **1996**, *35*, 5403–5406.
- [4] 10-Se-3 means that 10 electrons are formally associated with Se, to which 3 ligands are bonded: C. W. Perkins, J. C. Martin, A. J. Arduengo, W. Lau, A. Alegrie, J. K. Kochi, *J. Am. Chem. Soc.* **1980**, *102*, 7753–7759.
- [5] D. J. Williams, private communications.
- [6] A. J. Arduengo, E. M. Burgess, *J. Am. Chem. Soc.* **1977**, *99*, 2376–2378.
- [7] N. Kuhn, T. Kratz, G. Henkel, *Chem. Ber.* **1994**, *127*, 849–851.
- [8] W.-W. du Mont, *Main Group Chemistry News* **1994**, *2*, 18–26.
- [9] K. J. Wynne, P. S. Pearson, M. J. Newton, J. Golen, *Inorg. Chem.* **1976**, *15*, 1449–1451.
- [10] M. Bodelsen, G. Borch, P. Klæboe, P. H. Nielsen, *Acta Chem. Scand.* **1980**, *A34*, 125–139.
- [11] W. Gabes, D. J. Stufkens, H. Gerding, *J. Mol. Struct.* **1973**, *17*, 329–340.
- [12] A. I. Popov, R. F. Swensen, *J. Am. Chem. Soc.* **1955**, *77*, 3724–3726.
- [13] F. Demartin, F. A. Devillanova, F. Isaia, V. Lippolis, G. Verani, *Inorg. Chim. Acta* **1997**, *255*, 203–205.
- [14] N. Walker, D. Stuart, *Acta Crystallogr., Sect. A* **1983**, *39*, 158–166.
- [15] F. Uguzzoli, *Comput. Chem.* **1987**, *11*, 109–120.
- [16] G. M. Sheldrick, *SHELXS-86: Program for the Solution of Crystal Structures*, Universität Göttingen, Germany, **1986**.
- [17] *International Tables for X-ray Crystallography*; vol. IV, Kynoch Press, Birmingham, U.K., **1974**, 149, 99–102.
- [18] G. M. Sheldrick, *SHELX-76: Program for Crystal Structure Determination*, University of Cambridge, U.K., **1976**.
- [19] M. Nardelli, *Comput. Chem.* **1983**, *7*, 95–98.
- [20] C. K. Johnson, *ORTEP, Report ORNL-3794*, revised, Oak Ridge National Laboratory, Tennessee, **1965**.
- [21] W. D. S. Motherwell, PLUTO, University of Cambridge, U.K., **1976**.

[97152]